0888-8809/05/$15.00/0
Printed in U.S.A.

Molecular Endocrinology 19(3):683–697

doi: 10.1210/me.2004-0332

Proteomic Analysis Identifies Immunophilin FK506 Binding Protein 4 (FKBP52) as a Downstream Target of Hoxa10 in the Periimplantation Mouse Uterus

Takiko Daikoku, Susanne Tranguch, David B. Friedman, Sanjoy K. Das, David F. Smith, and Sudhansu K. Dey

Departments of Pediatrics (T.D., S.T., S.K.Da., S.K.De.), Cell and Developmental Biology, Pharmacology, Biochemistry (D.B.F.) and Cancer Biology (T.D., S.T., S.K.Da., S.K.De.), Division of Reproductive and Developmental Biology, Vanderbilt University Medical Center, Nashville, Tennessee 37232; and Department of Biochemistry and Molecular Biology (D.F.S.), Mayo Clinic, Scottsdale, Arizona 85259

The process of implantation absolutely requires synchronized development of the blastocyst to implantation competency, differentiation of the uterus to the receptive state, and a reciprocal dialogue between the blastocyst and uterine luminal epithelium. Genetic and molecular approaches have identified several signaling pathways that are critical to this process. The transcription factor Hoxa10 is one such critical player in implantation. *Hoxa10*$^{-/-}$ female mice have implantation and decidualization failure due specifically to reduced uterine responsiveness to progesterone and defective stromal cell proliferation during uterine receptivity and implantation. However, the downstream signaling pathways of Hoxa10 in these events remain largely unknown. Using the proteomics approach of difference gel electrophoresis, we have identified an immunophilin FKBP52 (FK506 binding protein 4) as one of the Hoxa10-mediated signaling molecules in the uterus. We found that FKBP52, a cochaperone protein known to influence steroid hormone receptor functions, is down-regulated in stromal cells of *Hoxa10*$^{-/-}$ mice. More importantly, FKBP52 shows differential uterine cell-specific expression during the periimplantation period. Whereas it is primarily expressed in the uterine epithelium on d 1 of pregnancy, the expression expands to the stroma on d 4 during the period of uterine receptivity and becomes localized to decidualizing stromal cells surrounding the implantation site on d 5. This suggests that FKBP52 is important for the attainment of uterine receptivity and implantation. Furthermore, FKBP52 shows differential cell-specific expression in the uterus in response to progesterone and/or estrogen consistent with its expression patterns during the periimplantation period. Collectively, these results and the female infertility phenotype of FKBP52 suggest that a Hoxa10-FKBP52 signaling axis is critical to uterine receptivity and implantation. (*Molecular Endocrinology* 19: 683–697, 2005)

HOX GENES ARE developmentally regulated transcription factors that belong to a multigene family. They share in common a highly conserved sequence element, called the homeobox, that encodes a 61-amino acid helix-turn-helix DNA-binding domain. Whereas one *Hox* cluster (the HOM-C) is present in *Drosophila*, four mammalian *Hox* clusters (a, b, c, and d) are present on different chromosomes and have evolved by gene duplication (1). These genes at the 3′-end of each cluster are activated during early embryogenesis in the anterior region of the developing embryo, whereas genes located toward the 5′-end are restricted to posterior regions of the embryo and are expressed during later stages of embryogenesis (1, 2). *AbdominalB* (*AdbB*) is the most 5′-gene within the *Drosophila* homeotic complex. In mammals, several *AbdB*-like genes exist at the 5′-ends of the Hox a, c, and d clusters corresponding to paralogous groups 9–13 (3). The *Adb* genes constitute a distinct subfamily of homeobox genes that exhibit posterior domains of expression including the genital imaginal disc in *Drosophila* and the developing genitourinary system in mammals (4, 5).

Hoxa10 is one *abdominalB*-like homeobox gene that is located in the *Hoxa* cluster and expressed in the developing genitourinary tract during mouse embryogenesis (3). Its distinct role in development has been

First Published Online November 4, 2004

Abbreviations: CHAPS, 3-[(3-Cholamidopropyl)dimethylammonio]-2-hydroxy-1-propanesulfonate; 2D, two-dimensional; DIGE, difference gel electrophoresis; DTT, dithiothreitol; E_2, 17β-estradiol; FBS, fetal bovine serum; FKBP52, FK506 binding protein 4; HBSS, Hanks' balanced salt solution; Hsp, heat shock protein; IPG, immobilized pH gradient; MALDI, matrix-assisted laser desorption/ionization; MS, mass spectrometry; P_4, progesterone; PDZ, primary decidual zone; PR, progesterone receptor; SDS, sodium dodecyl sulfate; SDZ, secondary decidual zone; TBST, Tris-buffered saline-Tween 20; TOF, time of flight.

***Molecular Endocrinology* is published monthly by The Endocrine Society (http://www.endo-society.org), the foremost professional society serving the endocrine community.**

defined by gene targeting experiments (6, 7). *Hoxa10*-deficient mice exhibit male and female infertility. The proximal region of the uterus in *Hoxa10*$^{-/-}$ mice shows partial homeosis into an oviduct-like structure. However, this is not the cause of infertility in these females. *Hoxa10* is strongly expressed in the mouse uterine stroma during the receptive phase, and also during implantation and the ensuing decidualization (7). Impaired stromal cell proliferation and decidualization are severely compromised in *Hoxa10*$^{-/-}$ mice, leading to pregnancy failure (8). Furthermore, embryo transfer experiments have conclusively shown the maternal requirement for Hoxa10 in both implantation and decidualization (7, 9).

Coordination between the establishment of uterine receptivity and implantation competency of the blastocyst is essential to the process of implantation. Ovarian progesterone (P_4) and estrogen play key roles in these processes. Whereas preovulatory estrogen secretion induces epithelial cell proliferation on d 1 of pregnancy, rising P_4 levels from the newly formed corpora lutea superimposed with ovarian estrogen secretion on d 4 directs stromal cell proliferation and epithelial cell differentiation, leading to uterine receptivity for implantation (10). We have previously shown that stromal cell proliferation in *Hoxa10*$^{-/-}$ mice in response to ovarian P_4 and estrogen is severely compromised, whereas epithelial cell proliferation remains normal in response to estrogen (9). These results provide evidence that stromal cell responsiveness to P_4 with respect to cell proliferation is impaired in *Hoxa10*$^{-/-}$ mice, and that Hoxa10 is intimately involved in mediating stromal cell proliferation. P_4 is a strong inducer of *Hoxa10* in the mouse uterine stroma, and its induction occurs in this uterine compartment within 4 h of P_4 injection in a protein synthesis-independent manner. The up-regulation of *Hoxa10* by P_4 is attenuated by the progesterone receptor (PR) antagonist RU-486, suggesting a requirement for PR in this induction (11). Collectively, these results suggest that Hoxa10 induces genes that are vital for stromal cell proliferation and differentiation in a P_4-dominant environment and that Hoxa10 functions as a mediator of P_4 effects in implantation. However, several P_4-responsive genes, such as *PR* itself, *Hoxa11*, and c-*myc*, respond normally to P_4 in *Hoxa10* null mice (9). Therefore the mechanism by which Hoxa10 regulates uterine stromal cell proliferation and differentiation during uterine receptivity, implantation, and decidualization still remains elusive.

In the present study, we first employed a differential-display proteomics analysis using two-dimensional (2D) difference gel electrophoresis (DIGE) on purified uterine stromal cells obtained from wild-type and *Hoxa10*$^{-/-}$ mice on d 4 of pseudopregnancy to compare differential expression profiles of proteins for identifying potential signaling targets of Hoxa10. DIGE provides a powerful quantitative component to conventional 2D gel electrophoresis and is capable of monitoring subtle abundance changes with statistical confidence owing to the ability to compare replicate measurements (12, 13). Sensitive and accurate matrix-assisted laser desorption/ionization (MALDI), time-of-flight (TOF), and tandem TOF/TOF mass spectrometry (MS), coupled with database interrogation, provided identification of 29 proteins with significant differences in expression levels. We focused on the immunophilin FKBP52 (FK506 binding protein 4) for further analysis because of its known assembly with multiple steroid hormone receptors (14) and its role regulating steroid hormone receptor function (15). Consistent with our proteomics data, we observed that the expression of FKBP52 is down-regulated in the stroma of *Hoxa10* mutant mice on d 4 of pseudopregnancy with unaltered expression in the luminal and glandular epithelia when compared with that of wild-type mice. We also observed that FKBP52 is uniquely expressed in the pregnant mouse uterus during the periimplantation period in a cell-specific manner. More importantly, FKBP52 expression in the stroma, but not in the epithelium, is regulated by P_4. These results suggest that the immunophilin FKBP52 is an important player in the P_4-Hoxa10 signaling axis in the periimplantation mouse uterus.

RESULTS

Stromal Cell-Specific Desmin and Vimentin Are Expressed in Cultured Cells

Because the uterus is comprised of heterogeneous cell types, analysis of protein profiles in whole uterine extracts will provide limited information. Fox example, the luminal epithelium represents about 5–10%, the stroma 30–35%, and the myometrium 60–65% of the major uterine cell types (16). Therefore, we sought to isolate pure stromal cells to compare protein expression profiles between *Hoxa10*$^{-/-}$ and wild-type mice by employing a previously described method (17, 18). It is to be noted that *Hoxa10* is expressed exclusively in uterine stromal cells on d 4 of pregnancy (7, 19). We used d 4 pseudopregnant uteri to avoid any contamination by blastocyst proteins. Because epithelial cells are unable to attach to the culture dish, pure stromal cells were obtained by removing the small number of contaminating floating epithelial cells from the cultures after 1 h of incubation. As shown in Fig. 1A, we observed no apparent morphological changes in stromal cells obtained either from wild-type or mutant uteri. However, as expected, stromal cell yield from the mutant uteri was much lower than that from the wild-type uteri. To confirm that the isolated cells were of stromal cell origin, we performed immunocytochemistry for two stromal cell markers, vimentin and desmin (20, 21). Indeed, almost all of the cultured cells obtained

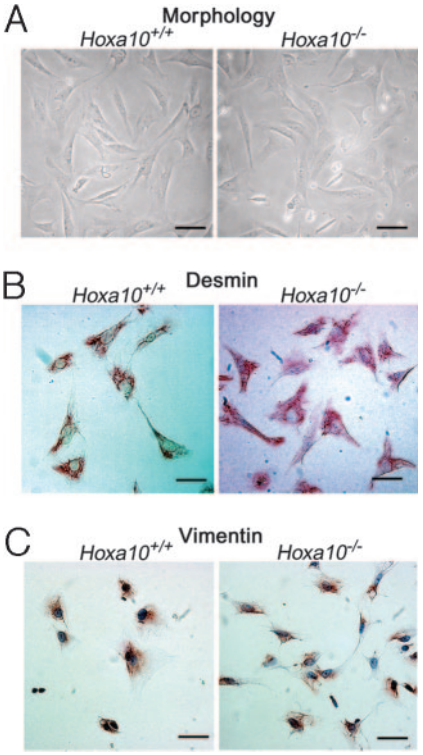

Fig. 1. Identification of Stromal Cell Purity

Enzymatically isolated uterine cells from *Hoxa10*$^{+/+}$ and *Hoxa10*$^{-/-}$ mice in culture expressed desmin and vimentin, the stromal cell-specific markers, providing evidence that the purified cells were of stromal cell origin. A, Morphology of cultured stromal cells. Immunostaining of desmin and vimentin in cultured cells is shown in panels B and C, respectively. *Bar*, 400 μm.

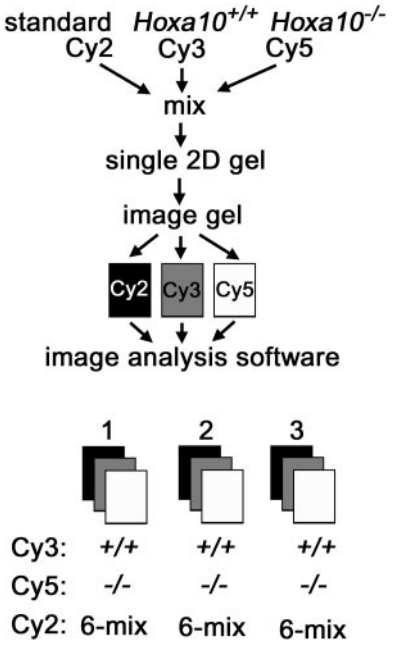

Fig. 2. A Schematic Representation of the 2D DIGE Analysis Performed, Using a Mixed Sample Internal Standard for the Identification of Differentially Expressed Proteins

Because the same mixture of samples is used for the standard and loaded onto each gel, quantitative comparisons can be made between the Cy3-labeled or Cy5-labeled protein signals relative to the Cy2-labeled standard, and then compared across triplicate gels for statistical confidence. Wild-type (+/+); Hoxa10$^{-/-}$ (−/−).

from wild-type or *Hoxa10*$^{-/-}$ uteri were desmin and vimentin positive (Fig. 1, B and C).

Stromal Cell Protein Profiles Are Different between Wild-Type and Hoxa10$^{-/-}$Mice

To determine which proteins are differentially expressed in wild-type *vs.* mutant stromal cells, we performed 2D DIGE analysis of proteins isolated from these cells after 24 h of culture. Triplicate protein extracts from wild-type or *Hoxa10*$^{-/-}$ stromal cells were labeled with the spectrally resolvable fluorescent Cy3 or Cy5 dyes, and Cy3/5 pairs were coresolved and independently imaged from three DIGE gels. A third dye (Cy2) was used to label a grand mixture of all six samples to provide an internal standard for each of the three DIGE gels, allowing for quantification of protein abundance changes with statistical confidence (Fig. 2; see *Materials and Methods*).

More than 1000 proteins were resolved with isoelectric points between pH 4 and 7 and molecular mass between 10 and 150 kDa. Among these, less than 4% (n = 36) of the detected features displayed changes in abundance that were consistent across all three measurements, supported by Student's *t* test *P* values within the 99th percentile confidence interval ($P < 0.01$, n = 3) for the variance of the mean changes (Fig. 3A and Tables 1 and 2). Twenty-two of these significant changes were in proteins up-regulated in *Hoxa10*$^{-/-}$ stromal cells, that include cytoskeletal, metabolic, and actin-related proteins such as fetuin-A, caldesmon, gelsolin, T-complex protein 1 (α-subunit B), and tropomyosin, displaying increases that range from 1.2- to 2.7-fold (Table 1). The seven down-regulated proteins in *Hoxa10*$^{-/-}$ stromal cells were mostly classified as metabolic with the exception of the FK506-binding protein 4 (FKBP52) that displayed a statistically significant decrease ($P = 0.00021$, Fig. 3, B and C, and Table 2). Peptide mass mapping and fragmentation spectra for FKBP52 are shown in Fig. 3, D–F. Seven targeted proteins failed to yield unambiguous protein identification in this study (data not shown); this could result from several factors, including relative abundance, distribution of trypsin cleavage sites and/or ionization efficiencies of recovered peptides.

We focused our attention to further characterize FKBP52 because of its interaction with steroid receptors, in particular progesterone receptor (PR) (14, 15, 22), and due to the potential influence of FKBP52 on receptor hormone binding affinity (23) and subcellular localization (24).

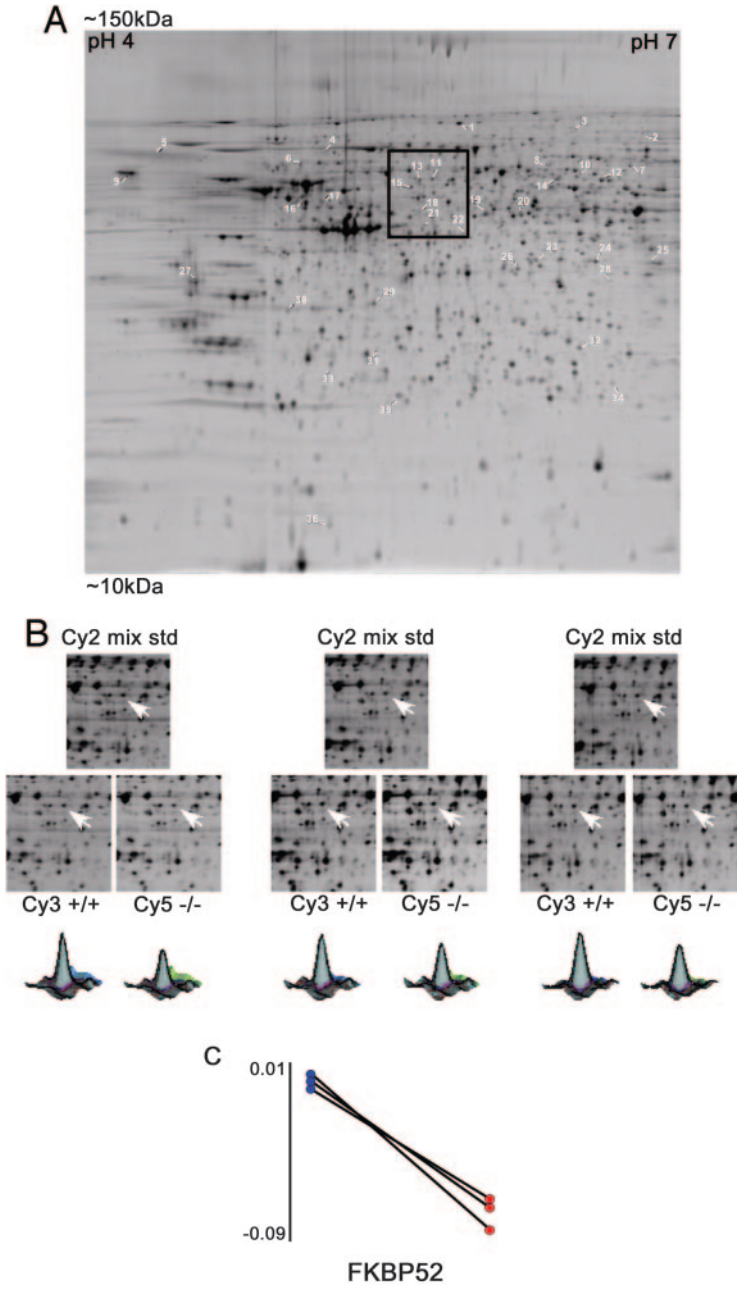

Fig. 3. 2D DIGE Analysis of Stromal Cells Isolated from *Hoxa10*$^{+/+}$ (+/+) *vs. Hoxa10*$^{-/-}$ (−/−) Uteri

A, Sypro Ruby poststain of one of the three coordinated DIGE gels, resolving proteins of isoelectric points between pH 4–7 and apparent molecular mass between approximately 10 and 150 kDa. *Numbered spots* correspond to proteins identified and listed in Tables 1 and 2. B, *Boxed region* in Sypro Ruby image *highlighted*, displaying the separate channels imaged from each gel: Cy2-labeled internal standard (comprising a mixture of all six samples, see *Materials and Methods*), Cy3-labeled *Hoxa10*$^{+/+}$ stromal cell extracts, and Cy5-labeled *Hoxa10*$^{-/-}$ stromal cell extracts. The *arrows* denote FKBP52 protein. Abundance levels of the Cy3 and Cy5 components of each gel are shown for FKBP52 protein as a three-dimensional representation of the pixel intensity of the signal across the protein. C, DeCyder 5.02 software was used to calculate abundance changes relative to the Cy2-labeled internal standard for every protein feature within each gel and across all three gels, yielding an average of 18% decrease in protein abundance for the FKBP52 protein in *Hoxa10*$^{-/-}$ cells ($P = 0.00021$; Student's *t* test). D, MALDI-TOF mass spectrum representing a peptide mass map of the FKBP52 protein. Ions labeled with an *asterisk* indicate peptide masses (M+H) that match predicted peptide masses for FKBP52, identified using the MASCOT search algorithm as described in *Materials and Methods*. MALDI-TOF/TOF tandem MS of the indicated ions is shown in panels E and F, with b-ion and y-ion cleavages that are consistent with the predicted amino acid sequence of the FKBP52-derived peptides depicted *above* and *below* the amino acid sequence, respectively.

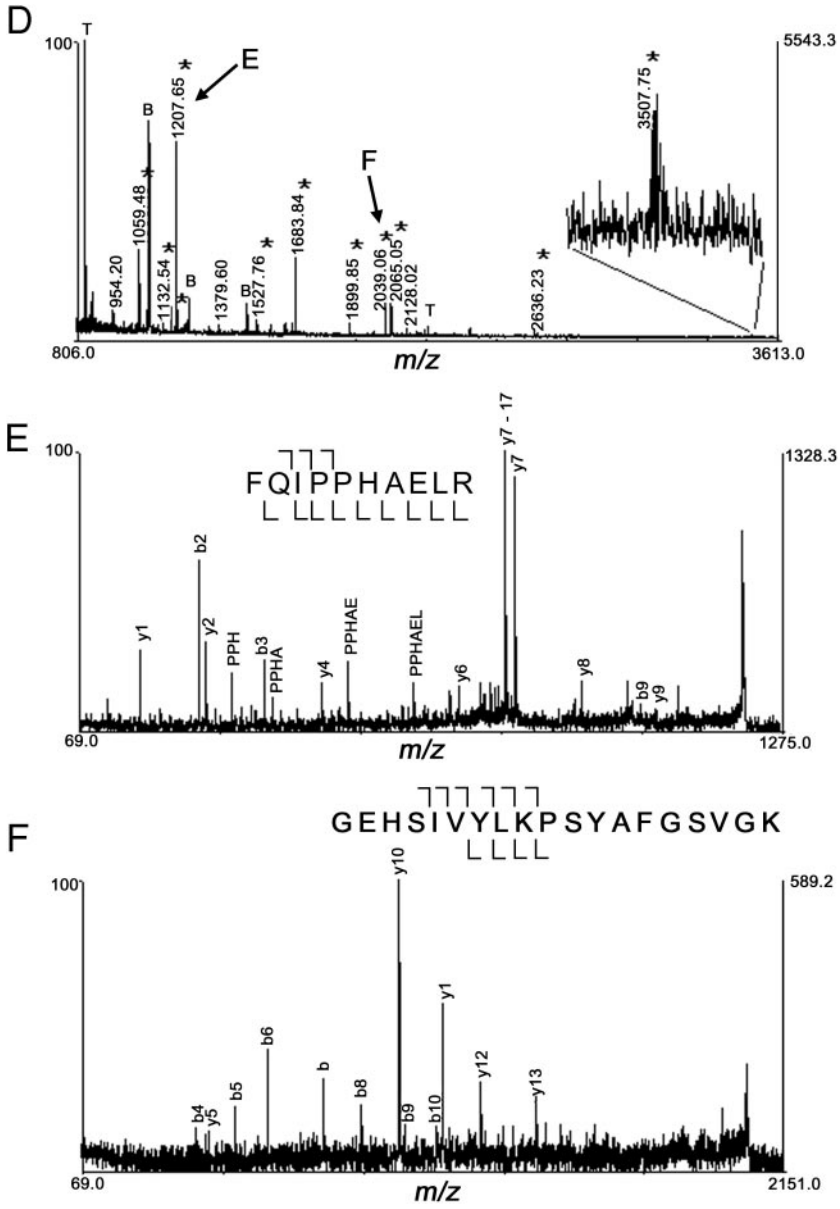

Fig. 3. *Continued*

Uterine FKBP52 Expression Is Cell Specific and Is Down-Regulated in Hoxa10$^{-/-}$ Mice

Our first objective was to confirm our proteomic data generated on isolated stromal cells with respect to *in vivo* expression of FKBP52 in uteri of wild-type and *Hoxa10*$^{-/-}$ mice. Immunostaining performed on sections of d 4 pseudopregnant mouse uteri showed that FKBP52 protein is present in the stroma as well as in the luminal and glandular epithelia in wild-type mouse uteri. However, its levels are low in the *Hoxa10*$^{-/-}$ uteri, especially in the stroma, when compared with wild-type uteri (Fig. 4A). Western blotting also detected the presence of FKBP52 protein in whole uterine extracts with higher levels in wild-type compared with *Hoxa10*$^{-/-}$ mice (Fig. 4B). However, when compared with actin levels, these changes are not especially dramatic. It should be noted that actin expression fluctuates in the rat and mouse uterus with changing experimental conditions (25, 26). Our present results also show fluctuation of several actin-binding proteins between *Hoxa10* mutant and wild-type stromal cells (Table 1). We next asked whether the localization of *FKBP52* mRNA follows the same pattern as the protein. Indeed, *in situ* hybridization showed that *FKBP52* mRNA expression follows the pattern of immunolocalization, and its expression is down-regulated in *Hoxa10*$^{-/-}$ uterine stroma (Fig. 4C). Collectively, these results confirm the proteomic data and provide further evidence that stro-

Table 1. Proteomic Identification of Up-Regulated Proteins in Uterine Stromal Cells of *Hoxa10*$^{+/+}$ *vs. Hoxa10*$^{-/-}$ Mice

Spot No.	Protein Name	GenBank Accession No.	Fold Change −/−:+/+ (n = 3)	*t* Test *P* Value (n = 3)	Functional Category
2	Nonmuscle caldesmon	Q62736 CALD_RAT	2.65	0.00017	Actin-binding protein
5	Fetuin A	P12763	2.45	1.80E-05	Cytoskeletal protein, antiinflammation
10 (mix)	Coronin-like protein and ATP-dependent RNA helicase DDX19	CO1A_MOUSE DD19_MOUSE	1.82	1.10E-05	Actin-related protein; RNA modification
20	Plasminogen/activator inhibitor-1	P22777 PAI1_MOUSE	1.59	0.00018	Inflammation
19	Plasminogen/activator inhibitor-1	P22777 PAI1_MOUSE	1.44	3.70E-05	Inflammation
24	Transaldolase	Q93092 TAL1_MOUSE	1.51	1.50E-05	Metabolism
32	Endoplasmic reticulum protein (ERp29)	P57759 Er29_MOUSE	1.48	4.30E-05	Chaperone
27	Tropomyosin	P58771 TPMI_MOUSE	1.43	0.00026	Actin-binding protein
1	Gelsolin	P13020 GELS_MOUSE	1.40	1.70E-06	Actin-binding protein
13	Aldehyde dehydrogenase	Q62148 DHA2_MOUSE	1.37	0.00054	Metabolism
4	Lamin B1	P14733 LAM1_MOUSE	1.35	0.0028	Glycoprotein, migration and proliferation
26	Transaldolase	Q93092 TAL1_MOUSE	1.33	8.30E-05	Metabolism
8	T complex protein 1 α-subunit B	P11983 TCP2_MOUSE	1.32	0.0018	Actin production
6	heteronuclearRNP K	O19049 ROK_RABBIT ROK_HUMAN	1.30	0.0019	RNA modification
29	Annexin A4	P97429 ANX4_MOUSE	1.30	0.00028	Cell aggregation
25	Annexin A1	P10107 ANX1_MOUSE	1.29	0.004	Antiinflammation
16	Protein disulfide isomerase A6	Q63081 PDA6_RAT	1.27	0.018	Calcium-binding protein
17	Protein disulfide isomerase A6	Q63081 PDA6_RAT	1.26	0.00047	Calcium-binding protein
30	Swiprosin 1	Q9D8Y0 SWS1_MOUSE	1.25	0.00061	Unknown
15	Cytosolic nonspecific dipeptidase	Q9D1A2 CGL1_MOUSE	1.24	0.00026	Protein modification
18	Eukaryotic initiation factor 4A-1	Gil50815 (MOUSE)	1.21	0.009	RNA translation

Uterine stromal cells from d 4 pseudopregnant uteri of wild-type or *Hoxa10*$^{-/-}$ mice were isolated by enzymatic digestion and cultured for 24 h. Protein profiles were generated by 2D-DIGE coupled with MS as described in *Materials and Methods.* Fold abundance changes are reported, whereby a fold increase is calculated directly from the Hoxa10 −/−:+/+ volume ratio, and a fold decrease = 1/volume ratio.

mal cell FKBP52 expression is compromised in uteri lacking Hoxa10.

FKBP52 Expression Correlates with Hoxa10 Expression in a Spatiotemporal Manner in the Periimplantation Uterus

Our next objective was to examine the temporal and cell-specific expression of *FKBP52* and *Hoxa10* before implantation (d 1 and d 4), at the time of implantation (d 5), and during the postimplantation (d 8) period (Fig. 5). The uterus is under the influence of preovulatory estrogen on d 1 of pregnancy or pseudopregnancy with heightened epithelial cell proliferation. In contrast, on d 4 the uterus is exposed to the rising levels of progesterone from the newly formed corpora lutea and fortified with a small amount of estrogen that results in epithelial cell differentiation with stromal cell prolifer-

Table 2. Proteomic Identification of Down-Regulated Proteins in Uterine Stromal Cells of *Hoxa10*$^{+/+}$ *vs. Hoxa10*$^{-/-}$ Mice

Spot No.	Protein Name	GenBank Accession No.	Fold change −/−:+/+ (n = 3)	*t* Test *P* Value (n = 3)	Functional Category
9	Calreticulin (ERp60)	P14211 CRTC_MOUSE	−1.39	0.00083	Chaperone
12	D-3-phosphoglycerate dehydrogenase	Q61753 SERA_MOUSE	−1.34	1.90E-05	Metabolism
14	D-3-phosphoglycerate dehydrogenase	Q61753 SERA_MOUSE	−1.30	0.0002	Metabolism
35	Adenylate kinase isozyme 1	Q9ROY5 KAD1_MOUSE	−1.31	0.0014	Metabolism
21	Succinyl-CoA ligase	Q9Z218 SCB2_MOUSE	−1.24	2.30E-05	Metabolism
11	FKBP52	P30416 FKB4_MOUSE	−1.22	0.00021	Chaperone
7	Asparagine synthetase	Q61024 ASNS_MOUSE	−1.20	0.0011	Metabolism

Procedures to isolate purified stromal cells and protein analysis are same as described for Table 1. CoA, Coenzyme A.

ation. The first molecular interaction between the blastocyst trophectoderm and the receptive uterus is observed at 1800 h on d 4 with the appearance of heparin-binding epidermal growth factor-like growth factor (HB-EGF) exclusively in the luminal epithelium surrounding the blastocyst. The first sign of the attachment reaction between the trophectoderm and luminal epithelium follows this event and occurs at 2200–2400 h on the same day (27). On the morning of d 5, the attachment between the luminal epithelium and the blastocyst trophectoderm is in the early stage with continued stromal cell proliferation and endometrial vascular permeability solely at the site of the blastocyst. The proliferating stromal cells surrounding the implanting blastocyst begin to differentiate to decidual cells from d 5 afternoon onward. On d 8, the implantation process is well advanced with maximal stromal cell decidualization (28). In mice, the proliferating and differentiating stromal cells surrounding the implanting blastocyst begin to form the primary decidual zone (PDZ) on d 5 afternoon. The PDZ is avascular and densely packed with decidual cells. By d 6, the PDZ is well formed and a secondary decidual zone (SDZ) is formed around the PDZ. At this time, cell proliferation ceases in the PDZ, but still continues in the SDZ (28). However, a thin layer of undifferentiated stromal cells establishes a boundary between the myometrium and SDZ. The PDZ progressively degenerates up to d 8. After d 8, the placental and embryonic growth gradually replaces the SDZ, which is reduced to a thin layer of cells called the decidua capsularis. The mesometrial decidual cells ultimately form the decidua basalis (28).

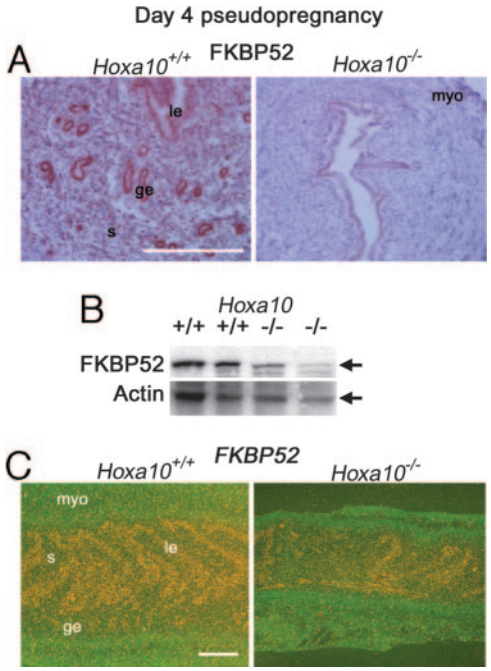

Fig. 4. Uterine Expression of FKBP52 in d 4 Pseudopregnant *Hoxa10*$^{+/+}$ and *Hoxa10*$^{-/-}$ Mice

A, Immunohistochemistry. Cross-sections of uteri were used for FKBP52 immunostaining (*bar*, 200 μm). B, Western blot analysis of FKBP52 (*arrow*); C, *in situ* hybridization. *FKBP52* expression in representative dark-field photomicrographs of longitudinal uterine sections is shown. *Bar*, 400 μm. le, Luminal epithelium; ge, glandular epithelium; s, stroma; myo, myometrium.

These characteristics of the periimplantation period led us to examine *FKBP52* and *Hoxa10* expression in parallel in the uterus on d 1, d 4, d 5, and d 8 of pregnancy by *in situ* hybridization (Fig. 5, A and B). We observed that *FKBP52* mRNA is detected mostly in the luminal epithelium on d 1 of pregnancy when the uterus is primarily under the influence of estrogen; *Hoxa10* expression in the uterus is minimal to undetectable on this day. On d 4, the expression expands into the stroma with its persistent expression in the luminal and glandular epithelia, suggesting that ovarian steroids coordinate this differential expression of *FKBP52*. *Hoxa10* expression on this day is prominent

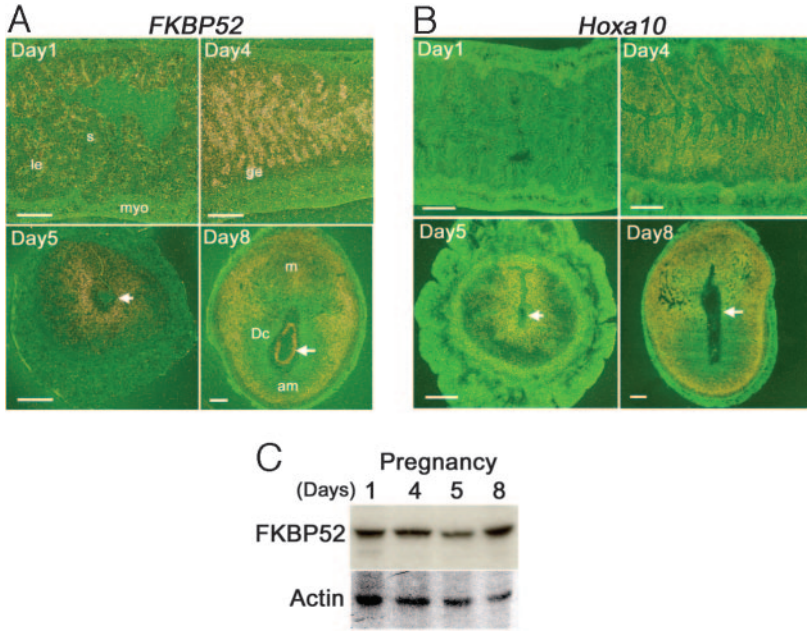

Fig. 5. Uterine Expression of FKBP52 and *Hoxa10* in Wild-Type Mouse Uteri during Early Pregnancy

In situ hybridization of *FKBP52* (panel A) and *Hoxa10* (panel B). Hybridization signals in representative dark-field photomicrographs of longitudinal uterine sections on d 1 and d 4 and cross-sections on d 5 and d 8 are shown. *Bar*, 200 μm. le, Luminal epithelium; ge, glandular epithelium; s, stroma; myo, myometrium; m, mesometrial pole; am, anti-mesometrial pole; Dc, decidua. *Arrows* indicate the location of embryos. C, Western blotting of FKBP52 protein.

in the stroma, but not in the epithelium. On d 5, the expression of both *FKBP52* and *Hoxa10* is uniquely displayed in the stroma surrounding the implanting blastocyst with little or no expression in the luminal epithelium. A low level of Hoxa 10 expression is also present in the circular smooth muscle on d 5. This suggests that the process of implantation has an impact on the expression of this immunophilin and Hoxa10. On d 8, their expression patterns dynamically change. *FKBP52* and *Hoxa10* are primarily expressed in peripheral decidualizing cells more specifically at the mesometrial SDZ and the undifferentiated stroma situated between the deciduum and myometrium. Interestingly, the expression of *FKBP52,* but not *Hoxa10,* is also evident in the growing embryo on this day. The results of Western blotting provided evidence that *FKBP52* mRNA is effectively translated in the uterus during these periods (Fig. 5C). Collectively, these results suggest that ovarian steroid hormones and events of implantation differentially regulate *FKBP52* and *Hoxa10* expression in the uterus.

Progesterone and Estrogen Differentially Regulate FKBP52 Expression in the Uterus

Our results showing differential expression of *FKBP52* on d 1 and d 4 of pregnancy suggested that this gene is regulated in the uterus by ovarian steroids in a cell-specific manner. Therefore, we further examined the expression of this gene in a more defined system, *i.e*. in ovariectomized mice after steroid hormone treatment. *In situ* hybridization was performed to determine uterine cell-specific expression of *FKBP52* in response to the ovarian steroid hormones P_4 and/or estrogen (Fig. 6A). We observed that *FKBP52* expression is low in uteri of ovariectomized mice treated with oil (vehicle control) and that this expression is primarily restricted to the luminal and glandular epithelia with low to undetectable expression in the stroma. An injection of 17β-estradiol (E_2, 100 ng/mouse) up-regulated the expression level by 12 h with the pattern remaining unaltered. In contrast, an injection of P_4 (2 mg/mouse) showed a prominent shift in the expression pattern from the luminal epithelium to the stromal cells at 12 h (Fig. 6A); the expression was down-regulated by 24 h (data not shown). A combined injection of E_2 and P_4 showed an expression pattern similar to that of P_4 alone but at somewhat lower levels (Fig. 6A). Interestingly, P_4 treatment markedly down-regulated the E_2 induced epithelial expression. Comparative RT-PCR analysis of total RNA isolated from uteri harvested from similarly treated mice confirmed the *in situ* hybridization results, showing an increase of *FKBP52* expression in E_2, P_4, and E_2 plus P_4 treatment at 12 h, with a return to basal levels at 24 h (Fig. 6B). To see whether steroid hormones influence *FKBP52* expression pattern in *Hoxa10* mutant mice, ovariectomized mutant mice were similarly treated with P_4 and/or E_2. The results show that the pattern of *FKBP52* expression mostly remains similar to those in wild-type mice at 12 h. However, *FKBP52* expression levels in *Hoxa10* mutant uteri are lower with the ex-

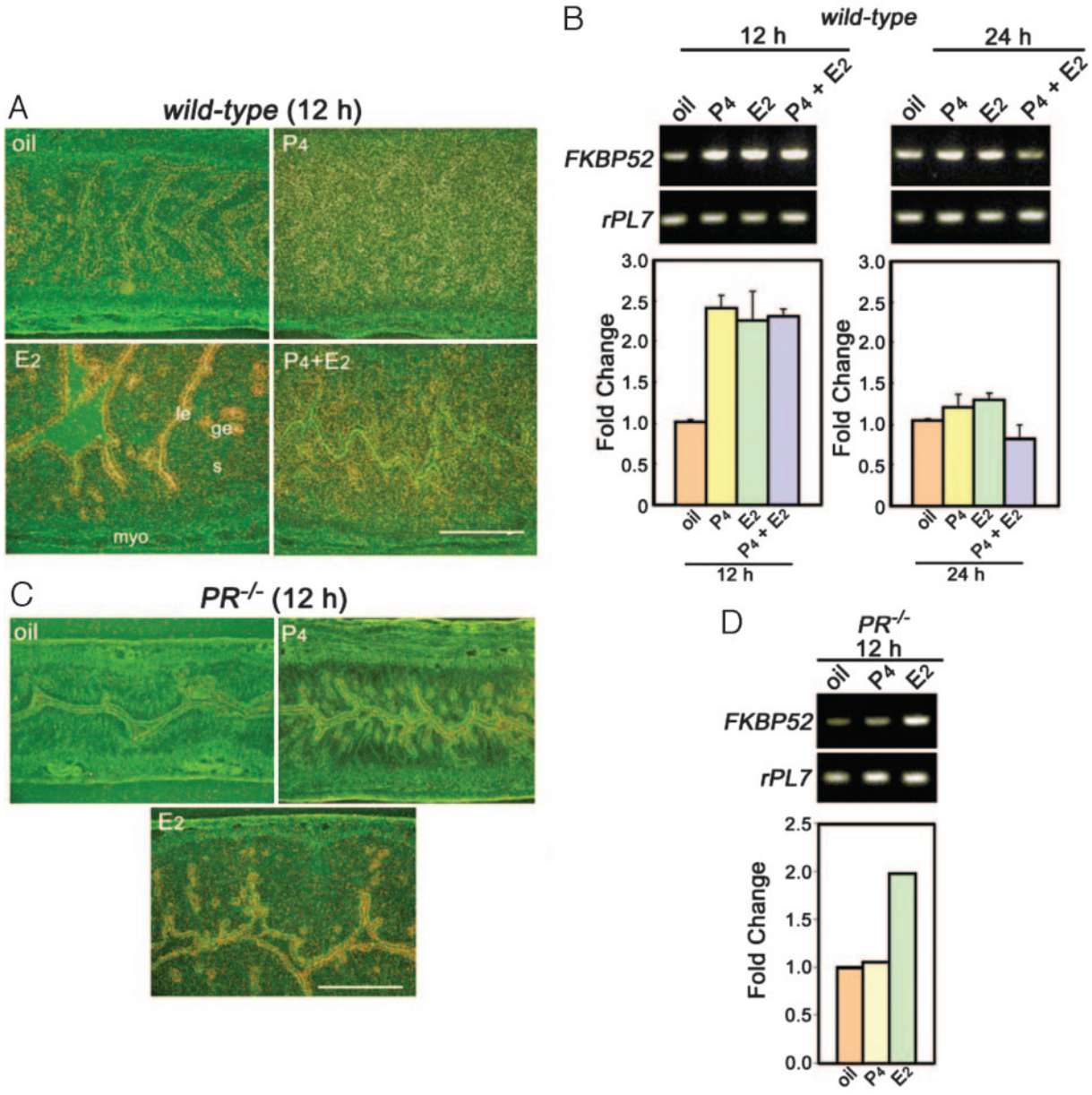

Fig. 6. Uterine *FKBP52* Expression in Ovariectomized Mice after Steroid Hormone Treatment

A, *In situ* localization of *FKBP52* mRNA in wild-type uteri is shown in representative dark-field photomicrographs of longitudinal uterine sections. Ovariectomized mice were treated with oil (control), E_2 (100 ng), P_4 (2 mg), or E_2+P_4 and killed at 12 h. *Bar*, 200 μm. le, Luminal epithelium; s, stroma; myo, myometrium. B, RT-PCR detection of *FKBP52* mRNA in wild-type uteri. Ovariectomized mice were treated with P_4 and/or E_2 for the indicated times. Total RNA was extracted and analyzed by comparative RT-PCR for *FKBP52* and *rpl7* as described in *Materials and Methods*. The data presented as fold induction are relative to oil treatment and are mean ± SE of three to four independent RNA samples except the 24 h E_2 treatment group in which two independent samples were used. C, *In situ* hybridization of *FKBP52* in $PR^{-/-}$ uteri. Ovariectomized mice were treated with oil (control), E_2 (100 ng), or P_4 (2 mg) and killed at 12 h. *Bar*, 200 μm. le, Luminal epithelium; s, stroma; myo, myometrium. D, RT-PCR detection of *FKBP52* in $PR^{-/-}$ uteri. Ovariectomized mice were treated with P_4 and/or E_2 at the indicated times.

ception of its higher levels in the epithelium after E_2 treatment similar to that observed in wild-type mice (Supplemental Fig. 1 published as supplemental data on The Endocrine Society's Journals Online web site at http://mend.endojournals.org). These results suggest that Hoxa10 influences P_4 regulation of FKBP52 in the stroma.

We next used mice lacking nuclear PR to further define the mechanism of steroidal regulation of *FKBP52*. The induction of stromal *FKBP52* expression that we observed in P_4-treated wild-type mice was virtually abolished in $PR^{-/-}$ mice (Fig. 6C). However, the E_2 response remained intact, showing a similar increase in *FKBP52* expression in the luminal epithe-

lium (Fig. 6C). The *in situ* hybridization results were further confirmed by comparative RT-PCR analysis of total RNA isolated from uteri harvested from similarly treated $PR^{-/-}$ mice, showing an increase in *FKBP52* expression with E_2 treatment, but no such increase in ovariectomized $PR^{-/-}$ mice treated with P_4 (Fig. 6D). In ovariectomized mice lacking the ERα gene, whereas E_2 treatment failed to induce epithelial expression of *FKBP52,* P_4 treatment induced its expression in the stroma (data not shown). Collectively, these results suggest that steroid hormones regulate *FKBP52* expression differentially and in a cell-specific manner.

DISCUSSION

Successful implantation absolutely depends on both the synchronized development of the blastocyst to the stage when it is competent to implant, and the uterus to the stage when it is receptive to blastocyst growth and implantation. Ovarian estrogen and P_4 are the primary effectors that direct the prereceptive uterus to a receptive state via a number of locally expressed growth factors, cytokines, transcription factors, and vasoactive mediators (28). Hoxa10 is well recognized as one of these mediators in the mouse uterus, especially in relation to P_4 signaling (11). However, the mechanism by which Hoxa10 regulates P_4-mediated uterine signaling relevant to implantation and decidualization still remains largely unknown.

Thus, our objective in this study was to identify signaling pathways related to Hoxa10 in the uterine stroma using 2D DIGE as a global proteomics approach because it is a valuable tool with which to generate a landscape of protein expression profiles. Our results show at least 36 proteins within the resolving power of the gels that are differentially expressed between $Hoxa10^{-/-}$ and wild-type uterine stromal cells with statistical confidence within the 99th percentile confidence interval (Student's *t* test, n = 3). This expression profile led us to focus on the relationship of FKBP52 with Hoxa10 and its regulation in the uterus with respect to uterine biology and implantation. In adult mice, P_4 priming is an absolute requirement for stromal cell proliferation in response to estrogen. Because this proliferation also requires the expression of Hoxa10, the down-regulation of FKBP52 in $Hoxa10^{-/-}$ mice reveals a potential downstream and integral target of Hoxa10 in this process. Steroid receptors are dependent on interactions with chaperone and cochaperone proteins to maintain their functions (29). Hormone-free steroid receptors assemble into heterooligomeric complexes with several molecular chaperone components, including the major heat shock protein Hsp90 and Hsp90-associated cochaperones such as FKBP52 or related immunophilins. The Hsp90-binding immunophilins are characterized by a tetratricopeptide repeat domain that targets the immunophilin to Hsp90-receptor complexes, plus a peptidylprolyl isomerase domain to which FK506 or other immunosuppressant drugs bind (30). FKBP52 and FKBP51 compete for a common binding site on Hsp90 and thus compete for assembly with receptor complexes. FKBP52 can elevate the hormone-binding affinity of glucocorticoid receptor in an Hsp90- and peptidylprolyl isomerase-dependent manner; conversely, FKBP51 can reverse the action of FKBP52 and revert glucocorticoid receptor to a lower affinity (23). FKBP51 expression is directly inducible by glucocorticoids (31) or P_4 (32, 33), and hormone-stimulated expression of this inhibitor can antagonize the actions of FKBP52, thus reducing secondary responses to hormones. Studies on New World primates, which display multihormone resistance and constitutively overexpress FKBP51, lend physiological support to the impact of FKBPs on steroid hormone receptors (34, 35). In a cDNA microarray approach to examine P_4-induced genes in the uterus of ovariectomized mice, *FKBP51* message was rapidly elevated followed by a subsequent elevation in *FKBP52* expression (36). The lagging up-regulation of *FKBP52*, presumably resulting from P_4-mediated induction of *Hoxa10*, might serve in part to compensate for elevated *FKBP51* expression and maintain PR sensitivity in uterine stromal cells. Indeed, our observation of the localization of FKBP52 in the uterus correlates well with that of PR (37). Estrogen has been shown previously to regulate FKBP52 expression in MCF-7 breast cancer cells (38).

The unique temporal and cell-specific localization of *FKBP52* in the mouse uterus during the periimplantation period suggests that this immunophilin is intimately involved with the dynamic changes in the uterus that occur during this period under the influence of ovarian steroids and locally produced paracrine, juxtacrine, and/or autocrine factors. Because P_4 effects are correlated with epithelial cell differentiation, but stromal cell proliferation on d 4, it is speculated that FKBP52 expression in the epithelium and stroma directs these events in the context of cell types. This is consistent with similar expression pattern of nuclear PR in the uterus on this day (37). This speculation is consistent with reduced *FKBP52* expression in $Hoxa10^{-/-}$ mice with reduced stromal cell proliferation. The expression of *PR*, *Hoxa10*, and *FKBP52* at similar sites of the stroma surrounding the implanting blastocyst on d 5 morning also suggest that Hoxa10, in association with FKBP52 under the influence of P_4, primarily promotes stromal cell proliferation, which is necessary for subsequent decidual growth. This is supported by the findings that implantation and decidualization are defective in the uterus lacking Hoxa10 (7, 9). Expression of *Hoxa10* and *FKBP52* in peripheral cells of the SDZ, especially at the mesometrial pole, again suggests that FKBP52-Hoxa10 signaling influences proliferation of decidualizing stromal cells. However, the potential function of FKBP52 and Hoxa10 that are expressed in the undifferentiated stroma on d 8 is not clearly understood. It is unknown how the decidual cell growth is restricted, leaving a

layer of undifferentiated stromal cells underneath the myometrium. Our recent results suggest that Wnt signaling plays a role in creating such a boundary in the uterus to prevent undifferentiated stromal cells from decidualization and restoring these undifferentiated precursor stromal cells for providing normal stromal tissue after the pregnancy is terminated (39). Whether FKBP52 in collaboration with Hoxa10 also plays a role in this event warrants further investigation.

Because P_4 priming of the uterus is a requirement for estrogen to initiate implantation in mice and because P_4 responsiveness is compromised in *Hoxa10*$^{-/-}$ mice (9), the down-regulation of FKBP52 in stromal cells lacking Hoxa10 suggests a functional role for a Hoxa10-FKBP52 signaling axis in uterine receptivity and implantation. This is consistent with a recent global gene expression profiling study that has shown initial down-regulation followed by up-regulation of *FKBP52* expression in the mouse uterus after P_4 treatment (36). In this respect, the ovariectomized mouse model provides a valuable experimental paradigm to study the effects of estrogen and/or progesterone on gene expression. Differential steroid hormonal regulation of *FKBP52* expression in a cell-specific pattern elucidates a possible signaling pathway between the epithelial and stromal compartments. Our findings of P_4 regulation of *FKBP52* expression in the stroma and that of estrogen in the epithelium suggest that different regulatory mechanisms are involved for differential cell-specific regulation. P_4 effects in the uterus are mediated by both PR-A and PR-B. Whether P_4 effects on uterine FKBP52 expression are mediated by PR-A, PR-B, or both will require further investigation. Nonetheless, the observation of differential regulation of FKBP52 by estrogen and P_4 points toward a role for FKBP52 in epithelial-mesenchymal cross-talk to mediate a full complement of uterine functions in response to ovarian steroid hormones. Our findings of lower levels of *FKBP52* expression in *Hoxa10* mutant uteri after P_4 treatment also suggest that optimal regulation of FKBP52 in the stroma by this steroid requires the presence of Hoxa10.

To elucidate a definitive role for FKBP52 in the uterus, however, requires genetic ablation of the gene. Indeed, *FKBP52* mutant mice have recently been generated, and preliminary characterization shows that homozygous deletion of this gene results in both male and female sterility. Female *FKBP52*$^{-/-}$ mice appear physically normal, but are infertile. Further analysis has shown that ovaries of *FKBP52* null mice appear morphologically normal with full oogenesis and follicular development. Furthermore, female mutant mice manifest normal ovulation and fertilization, and homozygous null embryos develop to the blastocyst stage. However, no sign of implantation or decidual swellings are apparent on d 8 of pregnancy, suggesting either failure of implantation or failure of decidualization immediately after implantation (D. Smith, manuscript in preparation). Therefore, infertility associated with these mice probably does not result from defects in oogenesis, ovulation, or fertilization, but could potentially occur at the implantation stage. This provides further evidence that the Hoxa10-FKBP52 axis is critical to implantation and decidualization.

This study recognizes proteomics analysis as a powerful tool with which to determine relevant players, which then can be further expounded by genetic and molecular approaches. The availability of *FKBP52* knockout mice will shed light regarding multifaceted roles of this protein in uterine receptivity, implantation, and decidualization. In this study, we also found other differentially regulated proteins between wild-type and *Hoxa10*$^{-/-}$ stromal cells. Future studies will clarify the role of these differentially expressed proteins in the mouse stroma and perhaps provide deeper insights into our understanding of uterine biology during preimplantation and decidualization.

MATERIALS AND METHODS

Gene-Targeted Mice

The disruption of the *Hoxa10* gene was performed by insertion of a neomycin resistance cassette into an *Xho*I site within the homeobox by homologous recombination in 129/SvJ embryonic stem (ES) cells as previously described (7). Richard L. Mass (Harvard Medical School) originally provided the *Hoxa10* mutant mice. Because *Hoxa10*$^{-/-}$ males are cryptorchids and infertile, *Hoxa10*$^{-/-}$ or wild-type females were mated with fertile or vasectomized wild-type males to induce pregnancy or pseudopregnancy (d 1 = vaginal plug), respectively. Estrogen receptor-α (ERα)-deficient mice (129/J/C57BL/6J) and PR-deficient mice (129SvEv/C57BL/6J) were generated as previously described (40, 41) and were kindly provided by Dennis Lubahn (University of Missouri, Columbia, MO) and Bert O'Malley (Baylor College of Medicine, Houston, TX), respectively, for establishing our colonies. PCR analysis of tail genomic DNA determined the genotypes. Mice used were housed in the institutional animal care facility according to National Institutes of Health and institutional guidelines on the care and use of laboratory animals.

Primary Culture of Uterine Stromal Cells

Procedures for the isolation and culture of mouse uterine stromal cells, collected on d 4 of pseudopregnancy, followed the previously described methods with minor modifications (17, 18). In brief, uteri were cleaned of fat tissue, slit longitudinally, and cut into small pieces (2–3 mm). Uterine pieces were then washed several times with phenol red-free Hanks' balanced salt solution (HBSS, Life Technologies, Gaithersburg, MD) with 100 μg/ml streptomycin, 100 U/ml penicillin, and 2.5 μg/ml amphotericin B (Sigma Chemical Co., St. Louis, MO). Tissues were digested with 6 mg/ml dispase (Life Technologies) and 25 mg/ml pancreatin (Sigma) for 1 h at 4 C, 1 h at room temperature, and 10 min at 37 C. After these digestion steps, tissues were immediately diluted in HBSS containing 10% fetal bovine serum (FBS) and mixed thoroughly to dislodge the sheet of luminal epithelial cells. The remaining tissues were washed twice in fresh medium (HBSS + antibiotics) and incubated again for subsequent digestion in fresh medium containing 0.5 mg/ml collagenase at 37 C for 30 min. At the end of digestion, tissues were immediately diluted in HBSS with 10% FBS and mixed thoroughly using a 25-ml pipette. The digested cells (primarily containing stro-

mal cells) were passed through a 70-μm nylon filter to eliminate any remaining clumps of epithelial cells and centrifuged. The pellet was washed twice with HBSS before the initiation of primary culture. Cells were plated and cultured in phenol red-free DMEM and Ham's F-12 nutrient mixture (1:1) with 10% charcoal-stripped serum and antibiotics. After an initial incubation for 1 h, the medium was removed along with free-floating cells, and the cells that remained adhered to the culture dishes were transferred to fresh medium (DMEM-F-12, 1:1) containing 10% charcoal-stripped FBS and antibiotics and cultured for 24 h in the absence of any steroid hormone.

2D DIGE

Cultured cells were washed with prechilled 1× PBS three times. RIPA buffer [150 mM NaCl, 1% Nonidet P-40, 0.5% deoxycholic acid, 0.5% sodium dodecyl sulfate (SDS), 50 mM Tris (pH 8)] was then added to make cell lysates. Cell lysates were centrifuged at 13,800 × *g* for 10 min at 4 C. Protein concentrations were measured using Bio-Rad Dc protein assay reagents (Bio-Rad Laboratories, Richmond, CA) in a photospectrometer. The mixed internal standard methodology (13, 42) was used in these studies with the following modifications. Six independent protein isolations were prepared from both wild-type and *Hoxa10*$^{-/-}$ mouse uterine stromal cells and cultured for 24 h as described above. Due to limited availability, all six *Hoxa10*$^{-/-}$ sample extracts were pooled (342 μg total) before precipitation with methanol-chloroform and resuspended in 171 μl buffer [7 M urea, 2 M thiourea, 4% 3-[(3-cholamidopropyl)dimethylammonio]-2-hydroxy-1-propanesulfonate (CHAPS), 30 mM Tris, 5 mM magnesium acetate] for a final concentration of 2 mg/ml. To be consistent, all six wild-type samples were similarly pooled (763.5 μg total) before precipitation and resuspension in 381.75 μl buffer. For each pooled sample, three independent 50 μl (100 μg) aliquots were labeled with either Cy3 or Cy5 (*N*-hydroxysuccinimidyl ester derivatives, GE Healthcare, Milwaukee, WI) as described below. The remaining *Hoxa10*$^{-/-}$ sample (21 μl, 42 μg) was then combined with 129 μl of wild-type sample (258 μg) to produce a 14:86 mixed-sample internal standard (300 μg total). Each 50 μl (100 μg) *Hoxa10*$^{-/-}$ and wild-type sample was separately labeled with 200 pmol of either Cy3 or Cy5 DIGE fluors (2 μl of a 100 pmol working solution in dimethyl formamide), and the 14:86 mixed-sample internal standard (300 μg total) was labeled with 600 pmol of Cy2. The stoichiometry of Cy-dye labeling was purposefully low to ensure equal labeling of the same protein from each extract, and the dyes exhibit a sensitivity that is at least that of conventional silver staining (~1 ng) under these conditions (43). Labeling was performed for 30 min on ice in the dark, after which the reactions were quenched with 2 μl of 10 mM lysine for every 200 pmol Cy-dye for 10 min on ice in the dark, followed by the addition of an equal volume of 2× rehydration buffer [7 M urea, 2 M thiourea, 4% CHAPS, 4 mg/ml dithiothreitol (DTT)] supplemented with 0.5% immobilized pH gradient (IPG) buffer 4–7. The samples were combined into tripartite Cy2/Cy3/Cy5-labeled mixtures such that each mixture had a wild-type 100 μg sample, a *Hoxa10*$^{-/-}$ 100 μg sample, and 100 μg of the Cy2-labeled internal standard (Fig. 2).

The three sets of tripartite-labeled samples were each brought to 450 μl final volume with rehydration buffer (7 M urea, 2 M thiourea, 4% CHAPS, 2 mg/ml DTT, 0.5% IPG buffer 4–7, trace bromophenyl blue, BPB) and were passively rehydrated into 24 cm 4–7 IPG strips (Amersham Biosciences, Arlington Heights, IL) for 28 h at room temperature in the dark. First-dimension isoelectric focusing was carried out for a total of 91 kVh, followed by second-dimension 12% SDS-PAGE using IPGphor and Ettan DALT 12 units, respectively (GE Healthcare). The isoelectrically focused samples were reduced and alkylated with DTT and iodoacetamide and equilibrated into the second dimension-loading buffer (glycerol, SDS, urea, trace BPB) according to the manufacturer's protocol. Second-dimension SDS-PAGE gels were precast with low-fluorescence glass plates, with one glass plate presilanized (bind-silane, GE Healthcare) to affix the polymerized gel to only one of the glass plates.

The Cy2, Cy3, and Cy5 components of each gel were individually imaged using mutually exclusive excitation/emission wavelengths of 488/520 nm for Cy2, 532/580 nm for Cy3, and 633/670 nm for Cy5 using a Typhoon 9410 Variable Mode Imager (GE Healthcare). After imaging for Cy-dye components, the nonsilanized glass plate was removed, and the gels were fixed in 50% methanol, 7% acetic acid for 2 h, and then incubated in Sypro Ruby in the dark overnight. This poststain visualizes approximately 97% of the unlabeled protein and ensures accurate protein excision, as the molecular weight and hydrophobicity of the Cy-dyes can influence protein migration during SDS-PAGE. Sypro Ruby images were acquired on the same imager using 457/610 nm wavelengths, as well as reimaged after excision to ensure accurate protein excision.

DIGE Analysis

DIGE technology provides relative quantification and statistical confidence in abundance changes of thousands of proteins resolved by 2D-gel separations (12, 13, 42–45). Using a pooled-sample internal standard present on each DIGE gel for normalization, many samples can be quantitatively intercompared across multiple DIGE gels that are run coordinately (13, 42), allowing for experimental replicates to be run simultaneously for statistical confidence.

DeCyder 5.02 software (Amersham Biosciences) was used for simultaneous comparison of abundance changes across all three sample pairs with statistical confidence. The DeCyder Differential In-gel Analysis (DIA) module was used for background normalization and triple codetection of the Cy2/Cy3/Cy5 signals for each resolved protein spot feature, after which Cy3:Cy2 and Cy5:Cy2 volume ratios were calculated. These ratios were used by the DeCyder Biological Variation Analysis module, which simultaneously matched all nine protein-spot maps from the three gels, and calculated average abundance changes and Student's *t* test *P* values for the variance of these ratios for each protein across all three DIGE gels. With this experimental design, all quantitative information is measured relative to the same internal standard present on all three gels, thereby allowing for the quantitative intercomparison of samples between the DIGE gels. Fold-abundance changes are reported, whereby a fold increase is calculated directly from the Hoxa10$^{-/-}$:Hoxa$^{+/+}$ volume ratio, and a fold decrease = 1/volume ratio.

Protein Identification by MS and Database Interrogation

Proteins of interest were robotically excised and processed for MALDI-TOF MS and TOF/TOF tandem MS using an Ettan Spot Handling Workstation (GE Healthcare). Briefly, gel plugs were excised and equilibrated with 50 mM ammonium bicarbonate and dehydrated with acetonitrile in a 96-well plate format. The proteins in the dehydrated gel plugs were digested in gel with 10 μl porcine modified trypsin protease (Promega Corp., Madison, WI) in 20 mM ammonium bicarbonate for 3 h at 37 C, and the resulting proteolytic peptides were extracted in two cycles of 60% acetonitrile-0.1% trifluoroacetic acid and dried. Peptides were reconstituted in 5 μl 60% acetonitrile-0.1% trifluoroacetic acid, and 0.5 μl of this mixture was applied to a MALDI target and mixed on target with 0.5 μl of α-cyano 4-hydroxycinnamic acid matrix (5 mg/ml in 60% acetonitrile-0.1% trifluoroacetic acid, supplemented with 1 mg/ml ammonium citrate). MALDI-TOF MS and TOF/TOF tandem MS were performed on a Voyager 4700 (Applied Biosystems, Foster City, CA) using data-dependent tandem MS acquisition on the 10 most abundant ions present

in each MALDI-TOF peptide mass map. MALDI-TOF peptide mass maps and accompanying tandem mass spectra were then collectively searched against the SWISS-PROT and NCBInr databases using GPS Explorer software (Applied Biosystems) running the MASCOT database search engine (Matrix-Science). MALDI-TOF peptide mass maps were internally calibrated to within 20 ppm mass accuracy using trypsin autolytic peptides (m/z = 842.51 and 2211.10). Searches were performed without constraining protein molecular weight or isoelectric point, and allowed for carbamidomethylation of cysteine, partial oxidation of methionine residues, and one missed trypsin cleavage. Identifications were accepted based on a tripartite evaluation that takes into account significant molecular weight search (MOWSE) scores, spectrum annotation, and observed *vs.* expected migration on the 2D gel (42).

Uterine Expression and Hormonal Regulation of FKBP52

In situ hybridization and immunohistochemistry were employed to examine the cell-specific expression of *FKBP52* mRNA and protein, respectively, in sections of d 4 pseudopregnant uteri from wild-type or *Hoxa10*$^{-/-}$ mice. To analyze *Hoxa10* and *FKBP52* expression in the uterus during the periimplantation period, wild-type uteri were collected in the morning (0900–1000 h) of d 1, d 4, d 5, and d 8 of pregnancy for *in situ* hybridization. To determine whether *FKBP52* was regulated by E_2 and P_4, wild-type, *PR*$^{-/-}$, *ER*$\alpha^{-/-}$, or *Hoxa*10$^{-/-}$ mice were ovariectomized and rested for 2 wk. They were treated with an injection of sesame oil (vehicle control; 0.1 ml/mouse), E_2 (100 ng/mouse), P_4 (2 mg/mouse), or a combination of E_2 and P_4. Mice were killed at indicated times, and uteri were collected for *in situ* hybridization and comparative RT-PCR.

Hybridization Probes

The cDNA clones for *FKBP52* were generated by RT-PCR cloning with specific primers. The cDNA clone for *Hoxa10* has been described previously (11). For *in situ* hybridization, sense and antisense ^{35}S-labeled cRNA probes were generated using *Sp6* and *T7* polymerases, respectively. Probes had specific activities of approximately 2×10^9 dpm/μg.

In Situ Hybridization

In situ hybridization was performed as previously described by us (27). In brief, frozen sections (12 μm) were mounted onto poly-L-lysine-coated slides and fixed in cold 4% paraformaldehyde in PBS. After prehybridization, the sections were hybridized at 45 C for 4 h in 50% formamide hybridization buffer containing the ^{35}S-labeled antisense or sense cRNA probes. Ribonuclease A-resistant hybrids were detected by autoradiography. Sections were poststained with eosin and hematoxylin. Sections hybridized with the sense probes did not exhibit any positive signals and served as negative controls.

Immunohistochemical Staining

Cultured mouse uterine stromal cells were stained for desmin- and vimentin-specific stromal cell markers in culture (20, 21). Cells were seeded in the chamber slides and cultured for 24 h and fixed in 10% formalin buffer. After washing in PBS, cells were immunostained by using an antibody against desmin (1:200) or vimentin (1:200, Santa Cruz Biotechnology, Inc., Santa Cruz, CA). The localization of FKBP52 in formalin-fixed paraffin-embedded uterine sections was achieved by following the protocol as previously described (19, 27). Immunostaining was performed using a polyclonal (rabbit) antibody to FKBP52. A Histostain-SP kit (Zymed Laboratories, Inc., South San Francisco, CA) was used for staining. Red deposits indicated the sites of positive immunostaining.

Western Blotting

Proteins were extracted from whole uterus on d 4 of pseudopregnancy and on d 1, d 4, d 5, and d 8 of pregnancy by homogenization in RIPA buffer containing proteinase and phosphatase inhibitor. The homogenates were centrifuged at 9800 $\times$ *g* for 10 min at 4 C. The supernatants were separated and their protein concentrations measured. The supernatants (50 μg protein) were then boiled for 5 min in SDS sample buffer. The samples were run on 10% SDS-PAGE gels under reducing conditions and transferred onto nitrocellulose membranes. The membranes were blocked with 10% milk in Tris-buffered saline-Tween 20 (TBST) for 1 h at room temperature and then incubated in 1% milk containing anti-FKBP52 antibodies (1:5000) overnight at 4 C. After incubation, membranes were washed three times (15 min each) with TBST, incubated with goat antirabbit IgG conjugated with horseradish peroxidase (1:20,000) in 1% milk at room temperature, and washed three times (15 min each) with TBST. The bands were detected using an enhanced luminescence kit (Amersham Pharmacia Biotech, Arlington Heights, IL).

RT-PCR

Total RNA was extracted from mouse uteri using Trizol according to the manufacturer's instruction. Reverse transcription with oligo(dT) priming was performed to generate cDNAs from 4 μg total RNA using Superscript II following the instruction provided by the manufacturer. DNA amplification was carried out with Taq DNA polymerase (Invitrogen, San Diego, CA) using the following primers: *FKBP52* (437 bp), 5′-AGT GTG GGG AAG GAG AGG TT-3′ and 5′-GCT CTT GCC AGG TCA AAG TC-3′; *rPL7* (246 bp), 5′-TCA ATG GAG TAA GCC CAA AG-3′ and 5′-CAA GAG ACC GAG CAA TCA AG-3′. PCR conditions were 95 C for 5 min and then 23 cycles of 94 C for 30 sec, 60 C for 30 sec, and 72 C for 45 sec, followed by incubation at 72 C for 10 min for *FKBP52* amplification. For *rPL7*, amplification was performed at 95 C for 5 min and then 23 cycles of 94 C for 30 sec, 60 C for 30 sec, and 72 C for 45 sec, followed by incubation at 72 C for 10 min. Amplified fragments were separated by electrophoresis on 2% agarose gels and visualized by ethidium bromide staining. The intensity of each band was measured by Scion Image (Scion Corp., Frederick, MD), and intensity of *FKBP52* was corrected by the intensity of *rPL7*.

Acknowledgments

We thank Salisha Hill and Corbin A. Williams for technical assistance in DIGE and protein identification.

Received August 24, 2004. Accepted October 27, 2004.

Address all correspondence and requests for reprints to: S. K. Dey, Department of Pediatrics, Vanderbilt University Medical Center, Nashville, Tennessee 37232. E-mail: sk.dey@vanderbilt.edu.

This work was supported in part by National Institutes of Health Grants HD12304, HD33994, HD37830, ES07814, DK48218, and CA77839). S. K. Dey is a recipient of Method to Extend Research in Time (MERIT) Awards from the National Institute of Child Health and Human Development (NICHD). Vanderbilt University provided institutional support through the Academic Venture Capital Fund.

REFERENCES

1. Krumlauf R 1994 Hox genes in vertebrate development. Cell 78:191–201
2. McGinnis W, Krumlauf R 1992 Homeobox genes and axial patterning. Cell 68:283–302
3. Benson GV, Nguyen TH, Maas RL 1995 The expression pattern of the murine Hoxa-10 gene and the sequence recognition of its homeodomain reveal specific properties of abdominal B-like genes. Mol Cell Biol 15: 1591–1601
4. Dolle P, Izpisua-Belmonte JC, Brown JM, Tickle C, Duboule D 1991 HOX-4 genes and the morphogenesis of mammalian genitalia. Genes Dev 5:1767–7
5. Izpisua-Belmonte JC, Falkenstein H, Dolle P, Renucci A, Duboule D 1991 Murine genes related to the *Drosophila* AbdB homeotic genes are sequentially expressed during development of the posterior part of the body. EMBO J 10:2279–2289
6. Rijli FM, Matyas R, Pellegrini M, Dierich A, Gruss P, Dolle P, Chambon P 1995 Cryptorchidism and homeotic transformations of spinal nerves and vertebrae in Hoxa-10 mutant mice. Proc Natl Acad Sci USA 92:8185–8189
7. Satokata I, Benson G, Maas R 1995 Sexually dimorphic sterility phenotypes in Hoxa10-deficient mice. Nature 374:460–463
8. Benson GV, Lim H, Paria BC, Satokata I, Dey SK, Maas RL 1996 Mechanisms of reduced fertility in Hoxa-10 mutant mice: uterine homeosis and loss of maternal Hoxa-10 expression. Development 122:2687–2696
9. Lim H, Ma L, Ma WG, Maas RL, Dey SK 1999 Hoxa-10 regulates uterine stromal cell responsiveness to progesterone during implantation and decidualization in the mouse. Mol Endocrinol 13:1005–1017
10. Huet-Hudson YM, Andrews GK, Dey SK 1989 Cell type-specific localization of c-myc protein in the mouse uterus: modulation by steroid hormones and analysis of the periimplantation period. Endocrinology 125: 1683–1690
11. Ma L, Benson GV, Lim H, Dey SK, Maas RL 1998 Abdominal B (AbdB) Hoxa genes: regulation in adult uterus by estrogen and progesterone and repression in mullerian duct by the synthetic estrogen diethylstilbestrol (DES). Dev Biol 197:141–154
12. Gade D, Thiermann J, Markowsky D, Rabus R 2003 Evaluation of two-dimensional difference gel electrophoresis for protein profiling. Soluble proteins of the marine bacterium *Pirellula* sp. strain 1. J Mol Microbiol Biotechnol 5:240–251
13. Alban A, David SO, Bjorkesten L, Andersson C, Sloge E, Lewis S, Currie I 2003 A novel experimental design for comparative two-dimensional gel analysis: two-dimensional difference gel electrophoresis incorporating a pooled internal standard. Proteomics 3:36–44
14. Tai PK, Maeda Y, Nakao K, Wakim NG, Duhring JL, Faber LE 1986 A 59-kilodalton protein associated with progestin, estrogen, androgen, and glucocorticoid receptors. Biochemistry 25:5269–5275
15. Barent RL, Nair SC, Carr DC, Ruan Y, Rimerman RA, Fulton J, Zhang Y, Smith DF 1998 Analysis of FKBP51/FKBP52 chimeras and mutants for Hsp90 binding and association with progesterone receptor complexes. Mol Endocrinol 12:342–354
16. Finn CA, Porter DG 1975 The uterus: cells and tissues of the endometrium. Acton, MA: Publishing Sciences Group, Inc.
17. Kover K, Liang L, Andrews GK, Dey SK 1995 Differential expression and regulation of cytokine genes in the mouse uterus. Endocrinology 136:1666–1673
18. Tan Y, Li M, Cox S, Davis MK, Tawfik O, Paria BC, Das SK 2004 HB-EGF directs stromal cell polyploidy and decidualization via cyclin D3 during implantation. Dev Biol 265:181–195
19. Lim H, Paria BC, Das SK, Dinchuk JE, Langenbach R, Trzaskos JM, Dey SK 1997 Multiple female reproductive failures in cyclooxygenase 2-deficient mice. Cell 91: 197–208
20. Glasser SR, Julian J 1986 Intermediate filament protein as a marker of uterine stromal cell decidualization. Biol Reprod 35:463–474
21. Piva M, Flieger O, Rider V 1996 Growth factor control of cultured rat uterine stromal cell proliferation is progesterone dependent. Biol Reprod 55:1333–1342
22. Smith DF, Baggenstoss BA, Marion TN, Rimerman RA 1993 Two FKBP-related proteins are associated with progesterone receptor complexes. J Biol Chem 268: 18365–18371
23. Riggs DL, Roberts PJ, Chirillo SC, Cheung-Flynn J, Prapapanich V, Ratajczak T, Gaber R, Picard D, Smith DF 2003 The Hsp90-binding peptidylprolyl isomerase FKBP52 potentiates glucocorticoid signaling in vivo. EMBO J 22:1158–1167
24. Pratt WB, Galigniana MD, Harrell JM, DeFranco DB 2004 Role of hsp90 and the hsp90-binding immunophilins in signalling protein movement. Cell Signal 16:857–872
25. Guo JZ, Gorski J 1988 Estrogen effects on histone messenger ribonucleic acid levels in the rat uterus. Mol Endocrinol 2:693–700
26. Wang XN, Das SK, Damm D, Klagsbrun M, Abraham JA, Dey SK 1994 Differential regulation of heparin-binding epidermal growth factor-like growth factor in the adult ovariectomized mouse uterus by progesterone and estrogen. Endocrinology 135:1264–1271
27. Das SK, Wang XN, Paria BC, Damm D, Abraham JA, Klagsbrun M, Andrews GK, Dey SK 1994 Heparin-binding EGF-like growth factor gene is induced in the mouse uterus temporally by the blastocyst solely at the site of its apposition: a possible ligand for interaction with blastocyst EGF-receptor in implantation. Development 120: 1071–1083
28. Dey SK, Lim H, Das SK, Reese J, Paria BC, Daikoku T, Wang H 2004 Molecular cues to implantation. Endocr Rev 25:341–373
29. Pratt WB, Toft DO 2003 Regulation of signaling protein function and trafficking by the hsp90/hsp70-based chaperone machinery. Exp Biol Med (Maywood) 228:111–133
30. Smith D 2004 Tetratricopeptide repeat cochaperones in steroid receptor complexes. Cell Stress Chap 9:109–121
31. Baughman G, Harrigan MT, Campbell NF, Nurrish SJ, Bourgeois S 1991 Genes newly identified as regulated by glucocorticoids in murine thymocytes. Mol Endocrinol 5:637–644
32. Hubler TR, Denny WB, Valentine DL, Cheung-Flynn J, Smith DF, Scammell JG 2003 The FK506-binding immunophilin FKBP51 is transcriptionally regulated by progestin and attenuates progestin responsiveness. Endocrinology 144:2380–2387
33. Kester HA, van der Leede BM, van der Saag PT, van der Burg B 1997 Novel progesterone target genes identified by an improved differential display technique suggest that progestin-induced growth inhibition of breast cancer cells coincides with enhancement of differentiation. J Biol Chem 272:16637–16643
34. Scammell JG, Denny WB, Valentine DL, Smith DF 2001 Overexpression of the FK506-binding immunophilin FKBP51 is the common cause of glucocorticoid resistance in three New World primates. Gen Comp Endocrinol 124:152–165
35. Reynolds PD, Ruan Y, Smith DF, Scammell JG 1999 Glucocorticoid resistance in the squirrel monkey is associated with overexpression of the immunophilin FKBP51. J Clin Endocrinol Metab 84:663–669

36. Yao MW, Lim H, Schust DJ, Choe SE, Farago A, Ding Y, Michaud S, Church GM, Maas RL 2003 Gene expression profiling reveals progesterone-mediated cell cycle and immunoregulatory roles of Hoxa-10 in the preimplantation uterus. Mol Endocrinol 17:610–627
37. Tan J, Paria BC, Dey SK, Das SK 1999 Differential uterine expression of estrogen and progesterone receptors correlates with uterine preparation for implantation and decidualization in the mouse. Endocrinology 140:5310–5321
38. Kumar P, Mark PJ, Ward BK, Minchin RF, Ratajczak T 2001 Estradiol-regulated expression of the immunophilins cyclophilin 40 and FKBP52 in MCF-7 breast cancer cells. Biochem Biophys Res Commun 284:219–225
39. Daikoku T, Song H, Guo Y, Riesewijk A, Mosselman S, Das SK, Dey SK 2004 Uterine Msx-1 and Wnt4 signaling becomes aberrant in mice with the loss of leukemia inhibitory factor or Hoxa-10: evidence for a novel cytokine-homeobox-Wnt signaling in implantation. Mol Endocrinol 18:1238–1250
40. Lubahn DB, Moyer JS, Golding TS, Couse JF, Korach KS, Smithies O 1993 Alteration of reproductive function but not prenatal sexual development after insertional disruption of the mouse estrogen receptor gene. Proc Natl Acad Sci USA 90:11162–11166
41. Lydon JP, DeMayo FJ, Funk CR, Mani SK, Hughes AR, Montgomery Jr CA, Shyamala G, Conneely OM, O'Malley BW 1995 Mice lacking progesterone receptor exhibit pleiotropic reproductive abnormalities. Genes Dev 9:2266–2278
42. Friedman DB, Hill S, Keller JW, Merchant NB, Levy SE, Coffey RJ, Caprioli RM 2004 Proteome analysis of human colon cancer by two-dimensional difference gel electrophoresis and mass spectrometry. Proteomics 4:793–811
43. Tonge R, Shaw J, Middleton B, Rowlinson r, Rayner S, Young J, Pognan F, Hawkins E, Currie I, Davison M 2001 Validation and development of fluorescence two-dimensional differential gel electrophoresis proteomics technology. Proteomics 1:377–396
44. Unlu M, Morgan ME, Minden JS 1997 Difference gel electrophoresis: a single gel method for detecting changes in protein extracts. Electrophoresis 18: 2071–2077
45. Gharbi S, Gaffney P, Yang A, Zvelebil MJ, Cramer R, Waterfield MD, Timms JF 2002 Evaluation of two-dimensional differential gel electrophoresis for proteomic expression analysis of a model breast cancer cell system. Mol Cell Proteomics 1:91–98

Molecular Endocrinology **is published monthly by The Endocrine Society (http://www.endo-society.org), the foremost professional society serving the endocrine community.**